

# Simultaneous Acquisition of $^{15}\text{N}$ - and $^{13}\text{C}$ -Edited NOE Spectra of Proteins Dissolved in $\text{H}_2\text{O}$

S. M. PASCAL,\*† D. R. MUHANDIRAM,\* T. YAMAZAKI,\*† J. D. FORMAN-KAY,† AND LEWIS E. KAY\*

\*Protein Engineering Network Centres of Excellence and Departments of Medical Genetics, Biochemistry and Chemistry, University of Toronto, Toronto, Ontario, Canada M5S 1A8; and †Division of Biochemistry Research, Hospital for Sick Children, 555 University Avenue, Toronto, Ontario, Canada M5G 1X8

Received October 21, 1993

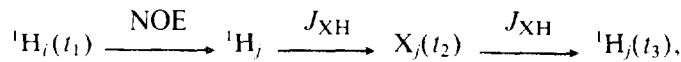
The development of multidimensional, multinuclear NMR spectroscopy has greatly simplified protein structure determination by NMR (1-8). NMR-derived structures are based, to a large extent, on distance restraints obtained from  $^{13}\text{C}$ - and  $^{15}\text{N}$ -edited 3D and 4D NOESY data sets recorded on both  $\text{H}_2\text{O}$  and  $\text{D}_2\text{O}$  samples as well as on torsion-angle restraints generated from a number of heteronuclear and homonuclear experiments (9, 10). At present, assignment of NOE data represents the most time-consuming step in the structure determination process. This is partially due to the necessity of examining a number of different NOE data sets in order to unambiguously assign the cross peaks. For example, the NOEs between aliphatic and NH protons in a 3D  $^{15}\text{N}$ -edited NOESY data set (11, 12) may be difficult to assign due to overlap of aliphatic  $^1\text{H}$  chemical shifts. An experiment which provides NOEs between  $^{15}\text{N}$ - and  $^{13}\text{C}$ -bound protons would both simplify the assignment process in this case and reduce the number of data sets that need be collected for a structure determination in general. While such information is available from the 4D  $^{15}\text{N}$ -,  $^{13}\text{C}$ -edited NOESY experiment (13), it is often at the expense of a considerable decrease in sensitivity relative to 3D data sets.

The incorporation of stereospecific assignments of  $\beta$ -methylene protons coupled with the use of specific ranges of allowed values for  $\phi$ ,  $\psi$ , and  $\chi_1$  torsion angles gives rise to increased precision in NMR-derived protein structures (9, 10). Intraresidue and sequential distances are required as input to conformational grid search routines which can provide torsion-angle restraints, as well as for stereospecific assignment of  $\beta$ -methylenes (14, 15). These distances can be obtained from short-mixing-time  $^{15}\text{N}$ - and  $^{13}\text{C}$ -edited NOESY experiments. An approach which gives NOEs to both  $^{15}\text{N}$ - and  $^{13}\text{C}$ -bound protons in the same experiment would decrease the measuring time necessary to obtain such information by a factor of two.

In this Communication, a pulse scheme is described, the CN NOESY-HSQC, which allows the simultaneous recording of  $^{15}\text{N}$ - and  $^{13}\text{C}$ -edited NOE spectra using an  $^{15}\text{N}$ ,  $^{13}\text{C}$ -labeled sample dissolved in  $\text{H}_2\text{O}$ . The simultaneous recording

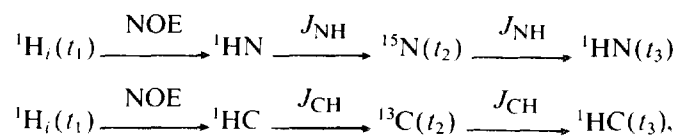
of  $^1\text{H}$  and  $^{13}\text{C}$  shifts in the context of a 3D HMQC-TOCSY experiment (16) and  $^{13}\text{C}$  and  $^{15}\text{N}$  chemical shifts in a  $^{15}\text{N}$ - $^{13}\text{C}$  HMQC experiment (17) have been described previously by Farmer and co-workers.

The transfer of magnetization in an X-edited NOE experiment ( $X = ^{15}\text{N}$  or  $^{13}\text{C}$ ) can be schematized by



where protons  $i$  and  $j$  are within approximately 5 Å.  $J_{\text{XH}}$  denotes the one-bond heteronuclear XH coupling constant, and the  $^1\text{H}_i$ ,  $\text{X}_j$ , and  $^1\text{H}_j$  chemical shifts evolve during  $t_1$ ,  $t_2$ , and  $t_3$ , respectively. In this experiment, phase cycling of one of the X pulses immediately before or after the  $t_2$  evolution period in a  $\pm$  manner with a concomitant inversion of the receiver phase results in the detection of protons that are one-bond-coupled to the heterospin, X. If  $X = ^{13}\text{C}$  and the sample is dissolved in  $\text{H}_2\text{O}$ , NOEs connecting all protons in the molecule (including NHs) to protons bound to  $^{13}\text{C}$  nuclei can be observed (18). Phase cycling eliminates the observation of signals emanating from the pathway whereby magnetization originating on any proton in the molecule is transferred via the NOE to nitrogen-bound protons. In order to observe these NOEs an  $^{15}\text{N}$ -edited NOESY experiment must also be recorded.

Figure 1 illustrates the pulse sequence that can be employed to simultaneously record  $^{15}\text{N}$ - and  $^{13}\text{C}$ -edited data sets. Because the pathways of transfer,



are independent, it is possible to select for both simultaneously by phase cycling  $\phi_2$  in Fig. 1 along with the receiver phase. A 3D data set is generated where each plane is labeled with either the  $^{15}\text{N}$  or the  $^{13}\text{C}$  chemical shift of the heteroatom

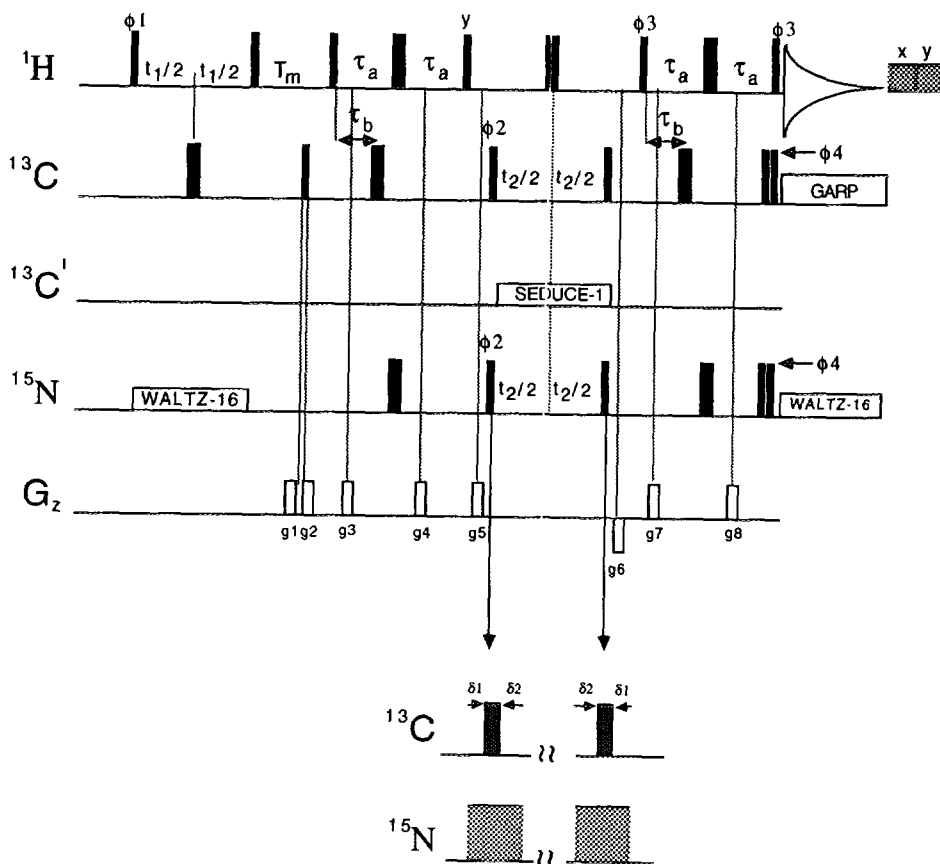


FIG. 1. Pulse sequence of the simultaneous  $^{15}\text{N}$ -edited and  $^{13}\text{C}$ -edited NOESY-HSQC experiment. Narrow (wide) pulses are applied with a flip angle of  $90^\circ$  ( $180^\circ$ ). All  $^1\text{H}$  pulses, with the exception of the  $x, y$  purge pulses immediately after acquisition (10 kHz field for 8 and 5 ms) are applied with a 21.7 kHz field. The  $^{13}\text{C}$  pulses were centered at 67 ppm and applied using an 18.5 kHz field. The first  $^{13}\text{C}$   $180^\circ$  pulse was applied as a composite pulse ( $90^\circ_x 180^\circ_y 90^\circ_x$ ). Decoupling of the  $\text{C}'$  spins was achieved using a 600 Hz SEDUCE-1 (21, 22) decoupling field centered at 175 ppm. A 3.5 kHz GARP (23) decoupling field was applied during acquisition. The GARP decoupling is preceded by high-power  $^{13}\text{C}$  and  $^{15}\text{N}$  pulse pairs as described previously (24).  $^{15}\text{N}$  decoupling during  $t_1$  and during acquisition was performed with a 1 kHz WALTZ-16 (25) decoupling field.  $^{13}\text{N}$  pulse widths of 47  $\mu\text{s}$  ( $90^\circ$ ) were employed. The delays used were  $\tau_a = \tau_b = 1.7$  ms and  $T_m = 150$  or 50 ms. The phase cycle  $\phi_1 = 4(x), 4(-x); \phi_2 = 8(x), 8(-x); \phi_3 = (x, y, -x, -y); \phi_4 = 4(x), 4(-x)$ ;  $\text{Rec} = (x, -y, -x, y, -x, y, x, -y, x, -y, -x, y)$  was employed. Quadrature in  $t_1$  and  $t_2$  was achieved via States-TPPI (24) of  $\phi_1$  and  $\phi_2$ , respectively. The durations and strengths of the gradients are:  $g1 = (2$  ms, 15 G/cm),  $g2 = (1$  ms, 20 G/cm),  $g3 = g4 = (1$  ms, 8 G/cm),  $g5 = (4$  ms, 30 G/cm),  $g6 = (3$  ms, -18 G/cm),  $g7 = g8 = (1$  ms, 8 G/cm). A delay of at least 50  $\mu\text{s}$  between the application of a gradient pulse and the subsequent application of an RF pulse is employed.

to which the destination proton is attached. Because  $^{15}\text{N}$ - and  $^{13}\text{C}$ -bound protons have distinct chemical shifts, with the possible exception of some  $\text{NH}/\text{NH}_2$  and aromatic protons, the extra information in these spectra relative to  $^{15}\text{N}$  or  $^{13}\text{C}$  data sets does not, in general, create ambiguities in interpretation. In order to simplify interpretation in cases where ambiguities may exist, the  $^{13}\text{C}$  carrier and carbon spectral width are adjusted so that cross peaks to aromatic protons are folded an odd number of times and therefore appear  $180^\circ$  out of phase relative to cross peaks to  $\text{NH}$  protons.

The CN NOESY-HSQC is very similar to the recently proposed gradient-NOESY-HSQC scheme for recording 3D  $^{13}\text{C}$ -edited NOESY data sets in  $\text{H}_2\text{O}$  (18) and many of the details of the present experiment, including the incorpo-

ration of pulsed field gradients to eliminate artifacts as well as to suppress the intense  $\text{H}_2\text{O}$  signal, are discussed elsewhere (18). In this Communication, we focus on the important differences between the present experiment and the  $^{13}\text{C}$  gradient-NOESY-HSQC. Because the values of  $J_{\text{NH}}$  and  $J_{\text{CH}}$  are somewhat different ( $J_{\text{NH}} \sim 92$  Hz and  $J_{\text{CH}}$  varies from  $\sim 125$  Hz for methyl groups to  $\sim 200$  Hz for aromatic residues), compromise delay values must be found for the transfer from a particular proton to its one-bond-coupled heterospin. In the sequence in Fig. 1, the transfer times for  $^1\text{H} \rightarrow ^{15}\text{N}$  and  $^1\text{H} \rightarrow ^{13}\text{C}$  are  $2\tau_a$  and  $2\tau_b$ , respectively, with  $\tau_b < \tau_a$  since  $J_{\text{CH}} > J_{\text{NH}}$ . Note, however, that transverse relaxation of  $^{15}\text{N}$ - and  $^{13}\text{C}$ -bound proton spins proceeds for the complete duration  $2\tau_a$  during each of the transfer steps in the sequence.

An important goal in the construction of the sequence in Fig. 1 was to adjust the timing delays in such a way so that cross peaks modulated by either  $^{15}\text{N}$  or  $^{13}\text{C}$  chemical shifts in  $t_2$  could be phased in this dimension using a first-order phase correction of  $180^\circ$ . In principle, this can be easily accomplished by setting the  $^{13}\text{C}$  and  $^{15}\text{N}$  pulse widths to be identical. However, the large carbon bandwidth requires the use of the largest RF field possible for carbon pulses, typically 18–19 kHz on our spectrometer. This is approximately a factor of three greater than the maximum field strength available for  $^{15}\text{N}$  pulses. Nevertheless, a  $180^\circ$  first-order phase correction in  $F_2$  can be obtained for both  $^{15}\text{N}$ - and  $^{13}\text{C}$ -modulated data using the timing diagram indicated at the bottom of Fig. 1. In this case, the  $^{13}\text{C}$  and  $^{15}\text{N}$  pulses are not centered; rather the first  $^{13}\text{C}$  pulse, of duration  $\text{pwc}$ , commences at  $\delta_1 = [(\pi/2)/\pi] \times (\text{pwn} - \text{pwc})$  after the start of the  $^{15}\text{N}$   $\phi_2$  pulse of duration  $\text{pwn}$ , while the  $^{13}\text{C}$  pulse immediately after the  $t_2$  evolution period begins at  $\delta_2 = (2/\pi) \times (\text{pwn} - \text{pwc})$  after the start of the corresponding  $^{15}\text{N}$  pulse. By setting the initial  $t_2$  value,  $t_2(0) = 1/(2 \text{SW}_2) - [\{4/\pi\} \text{pwn} + 2\text{pw}]$ , where  $\text{SW}_2$  is the spectral width in the  $^{13}\text{C}$  and  $^{15}\text{N}$  dimensions and  $\text{pw}$  is the  $^1\text{H}$   $90^\circ$  pulse width, a  $180^\circ$  first-order phase correction in  $F_2$  is obtained. Note that identical spectral widths are employed for both  $^{13}\text{C}$  and  $^{15}\text{N}$ . Farmer has derived identical results for the simultaneous  $^{15}\text{N}$ ,  $^{13}\text{C}$  HMQC experiment (17).

A novel feature of the resulting data set, originating from the fact that NOEs to both  $^{15}\text{N}$ - and  $^{13}\text{C}$ -bound protons are present, is that for each NOE between a carbon-bound proton and a nitrogen-bound proton at ( $\nu_{\text{CH}}$ ,  $\nu_{\text{N}}$ ,  $\nu_{\text{NH}}$ ) it is possible to find a “symmetry-related” cross peak at ( $\nu_{\text{NH}}$ ,  $\nu_{\text{C}}$ ,  $\nu_{\text{CH}}$ ), where  $\nu_{\text{CH}}$  and  $\nu_{\text{NH}}$  are the carbon-bound proton and nitrogen-bound proton chemical shifts, and  $\nu_{\text{C}}$  and  $\nu_{\text{N}}$  are the shifts of the directly attached  $^{13}\text{C}$  and  $^{15}\text{N}$  nuclei, respectively. Symmetry peaks are also present for NOEs between two nitrogen-bound protons or carbon-bound protons, as well. Locating these peaks is made particularly straightforward through the use of the PIPP program written by D. Garret at the NIH (19), which generates a list of possible symmetry-related cross peaks for any given peak in a data set. Thus, four chemical shifts, for the two protons and the two directly attached heteroatoms, can potentially be derived for each NOE. Of course, this information is also available from a combination of 3D or 4D  $^{15}\text{N}$ - and  $^{13}\text{C}$ -edited NOESY data sets as well as a 4D  $^{15}\text{N}$ ,  $^{13}\text{C}$  NOESY. Specifically, the four chemical shifts necessary for unambiguous assignment of an NOE between a carbon-bound proton and a nitrogen-bound proton are provided in the 4D  $^{15}\text{N}$ ,  $^{13}\text{C}$  NOESY. However, in the present application we have found that the use of a single CN NOESY-HSQC data set provides a rapid and straightforward approach for the unambiguous assignment of most of the NOEs between aliphatic and amide protons.

$^{15}\text{N}$ ,  $^{13}\text{C}$ -edited NOESY-HSQC experiments were recorded on a 1.5 mM,  $^{15}\text{N}$ ,  $^{13}\text{C}$ -labeled sample of a 105-amino-acid

fragment comprising the C-terminal SH2 domain from phospholipase C $_{\gamma 1}$  (PLC $_{\gamma 1}$ ) in a 1:1 complex with a 12-residue target phosphorylated peptide, pY1021, from the Y1021 site of the platelet-derived growth-factor receptor (PDGFR). The sample conditions used were pH 6.3, 0.1 M sodium phosphate, 90%  $\text{H}_2\text{O}$ /10%  $\text{D}_2\text{O}$ , and  $T = 30^\circ\text{C}$ . The experiment was performed on a Varian UNITY 500 MHz spectrometer equipped with a pulsed-field-gradient unit and an actively shielded triple-resonance probe head. Only  $z$  gradients of rectangular shape were employed.

Figure 2 illustrates the quality of the data obtained using the present sequence with a mixing time of 150 ms. Symmetry-related NOEs are shown for cross peaks connecting Leu-77  $\text{C}^\alpha\text{H}$  with Leu-80 NH in Figs. 2a and 2b and Ile-55  $\text{C}^\delta\text{H}$  with Met-26 NH in Figs. 2c and 2d. It would not be possible to assign these NOEs uniquely from an  $^{15}\text{N}$ -edited data set alone. In the case of the Ile-55–Met-26 NOE, for example, there are four methyl groups from residues Leu-35, Leu-16, Ile-55, and Val-67 with proton chemical shifts between 0.66 and 0.72 ppm. In addition to NOEs between amide and aliphatic or aromatic protons, the experiment also provides NOEs between exclusively  $^{13}\text{C}$ -bound or  $^{15}\text{N}$ -bound protons. Examples of these classes of NOEs are also observed in the figure.

In Fig. 3, slices showing  $\text{NH}-\text{C}^\beta\text{H}$  and  $\text{C}^\alpha\text{H}-\text{C}^\beta\text{H}$  cross peaks from a 50 ms-mixing-time data set are presented for residues Y84 and M68. The relative intensities of the cross peaks are used as input into a conformational grid search program along with coupling-constant information to provide stereospecific assignments and torsion-angle restraints (14, 15). Normally this information would be extracted from short-mixing-time  $^{15}\text{N}$ - and  $^{13}\text{C}$ -edited data sets, which in total require twice the measuring time as the present experiment. The data presented here along with the results obtained from a variety of other experiments indicate that both Y84 and M68 have  $\chi_1$  values of  $\sim -60^\circ$  and allow the stereospecific assignments given in the figure to be made.

The advantages associated with this experiment do come at a cost, unfortunately. In the present applications, we have opted to maximize the intensity of  $^{13}\text{C}$ -modulated cross peaks at the expense of some sensitivity loss in the  $^{15}\text{N}$ -edited spectrum by choosing  $\tau_a = \tau_b = 1.7$  ms. With the values of  $\tau_a$  and  $\tau_b$  chosen,  $^{13}\text{C}$ -edited cross peaks will be of the same intensity as those observed in the gradient  $^{13}\text{C}$ -edited NOESY-HSQC experiment described previously (18). However, relative to a  $^{15}\text{N}$ -edited NOESY-HSQC experiment, a sensitivity loss of approximately 20% is calculated for cross peaks to NH protons, assuming NH linewidths of 15 Hz. This estimate does not include the effects of the additional relaxation pathways provided by  $^{13}\text{C}$  labeling, which will decrease the sensitivity and the resolution of the  $^{15}\text{N}$ -edited spectrum still further. In this context, it is important to point out that the resolution available in  $F_2$  is governed by the minimum spectral width needed to accommodate the

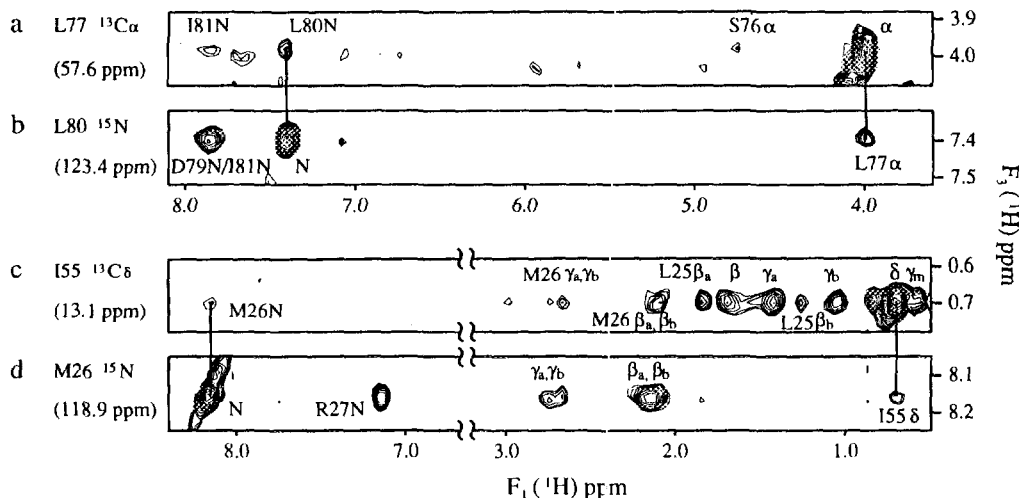


FIG. 2. Slices from a 150 ms-mixing-time simultaneous  $^{15}\text{N}$ -edited and  $^{13}\text{C}$ -edited NOESY-HSQC data set recorded on the  $\text{PLC}_{\gamma 1}$  SH2-pY1021 complex showing pairs of "symmetry-related" cross peaks for NOEs between  $\text{L80NH}$  and  $\text{L77C}^{\text{a}}\text{H}$  (a, b) and  $\text{M26NH}$  and  $^{15}\text{C}^{\text{d}}\text{H}$  (c, d). The cross peaks are observed on planes with the appropriate  $F_2$  chemical shift being that of either  $^{15}\text{N}$  or  $^{13}\text{C}$  depending on whether the destination proton is an amide or aliphatic proton. The cross peak of interest from each slice is connected to the diagonal on the corresponding slice by a vertical line. Peaks are labeled with the atom name and interresidue NOEs are additionally labeled with the residue. The spectrum was recorded as a  $128 \times 32 \times 416$  complex data matrix with acquisition times of 25.6, 10.7, and 52 ms in  $t_1$ ,  $t_2$ , and  $t_3$ , respectively. The data set was processed to give a final absorptive spectrum consisting of  $256 \times 128 \times 1024$  points. In order to optimize the resolution of the  $^{15}\text{N}$  lines, linear prediction was employed in  $t_2$ . The intensity of the residual water signal was minimized through the use of a time-domain deconvolution procedure discussed previously (18).

large dispersion of carbon chemical shifts. Although extensive folding of carbon resonances is employed, a minimum spectral width of  $\sim 3$  kHz is needed in  $F_2$  to allow unambiguous interpretation of NOEs. This limits the resolution available for  $^{15}\text{N}$ -edited cross peaks to approximately one-half the resolution that would normally be present in  $^{15}\text{N}$ -edited data sets, necessitating the use of linear prediction in the  $t_2$  dimension. Despite the decreased sensitivity relative to an op-

timized  $^{15}\text{N}$ -edited NOESY, the CN NOESY-HSQC experiment will have better sensitivity than the  $^{15}\text{N}$ ,  $^{13}\text{C}$ -edited 4D NOESY since magnetization is transferred from protons to  $^{15}\text{N}$  and  $^{13}\text{C}$  spins simultaneously, rather than sequentially, thereby decreasing the relaxation losses significantly. Indeed, the sensitivity of the CN NOESY-HSQC experiment is significantly higher than that of the 4D  $^{15}\text{N}$ ,  $^{13}\text{C}$  NOE experiment for  $\text{PLC}_{\gamma 1}$  SH2.

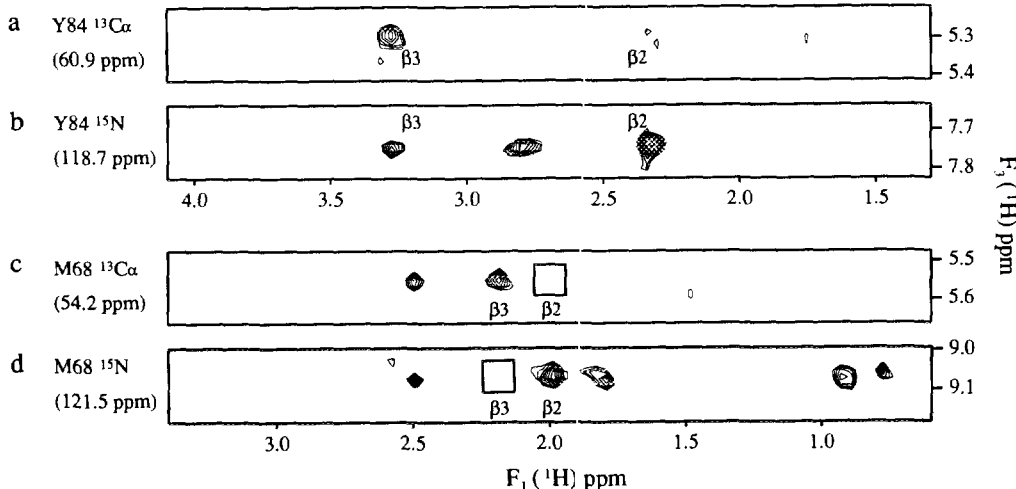


FIG. 3. Slices from a 50 ms-mixing-time simultaneous  $^{15}\text{N}$ -edited and  $^{13}\text{C}$ -edited NOESY-HSQC data set recorded on the  $\text{PLC}_{\gamma 1}$  SH2-pY1021 complex. Intraresidue  $\text{NH}-\text{C}^{\text{a}}\text{H}$  and  $\text{C}^{\text{a}}\text{H}-\text{C}^{\text{b}}\text{H}$  cross peaks for residues Y84 and M68 are indicated. Boxes indicate the position of the missing  $\text{NH}-\text{C}^{\text{a}}\text{H}$  or  $\text{C}^{\text{a}}\text{H}-\text{C}^{\text{b}}\text{H}$  NOEs. Processing was identical to that in the 150 ms data set (Fig. 2).

Although improved suppression of water can be achieved with the use of schemes involving a combination of selective RF pulses to excite the water resonance and gradient pulses (20), this has not been employed in the present application since the use of such approaches decreases the intensity of cross peaks originating from labile protons or protons with chemical shifts proximate to the water resonance. Residual water is removed efficiently in a postacquisition manner using a time-domain deconvolution procedure discussed previously (18).

In summary, a pulse scheme allowing the simultaneous recording of <sup>15</sup>N-edited and <sup>13</sup>C-edited NOESY-HSQC spectra of <sup>15</sup>N, <sup>13</sup>C-labeled proteins dissolved in H<sub>2</sub>O is presented. NOEs between all protons in the molecule are observed in a single data set. The compromise in sensitivity and resolution relative to <sup>15</sup>N-edited or <sup>13</sup>C-edited spectra recorded separately with delays chosen to optimize the appropriate magnetization transfers is offset by the ease of data analysis and the net reduction in acquisition time required to record all of the NOE information necessary for a structure determination.

#### ACKNOWLEDGMENTS

We thank Alex Singer for preparing the PLC<sub>γ1</sub> SH2 sample used in this study and Steve Shoelson, Harvard University, for the generous gift of the pY1021 phosphopeptide. This work was supported through grants from the Natural Sciences and Engineering Research Council of Canada (L.E.K.) and the National Cancer Institute of Canada (J.D.F. and L.E.K.) with funds from the Canadian Cancer Society. S. M. Pascal and Toshio Yamazaki are the recipients of postdoctoral fellowships from the Medical Research Council of Canada and the Human Frontiers Science Program, respectively.

#### REFERENCES

1. M. Ikura, L. E. Kay, and A. Bax, *Biochemistry* **29**, 4659 (1990).
2. L. E. Kay, M. Ikura, R. Tschudin, and A. Bax, *J. Magn. Reson.* **89**, 496 (1990).
3. G. T. Montelione and G. Wagner, *J. Magn. Reson.* **87**, 183 (1990).
4. R. T. Clubb, V. Thanabal, and G. Wagner, *J. Biomol. NMR* **2**, 203 (1992).
5. S. Grzesiek and A. Bax, *J. Magn. Reson.* **96**, 432 (1992).
6. B. T. Farmer, R. A. Venters, L. D. Spicer, M. G. Wittekind, and L. Mueller, *J. Biomol. NMR* **2**, 195 (1992).
7. A. G. Palmer, W. J. Fairbrother, J. Cavanaugh, P. E. Wright, and M. Rance, *J. Biomol. NMR* **2**, 103 (1992).
8. S. Grzesiek and A. Bax, *J. Am. Chem. Soc.* **114**, 6291 (1992).
9. G. Wagner, *Methods Enzymol.* **176**, 93 (1989).
10. G. M. Clore and A. M. Gronenborn, *Science* **252**, 1390 (1991).
11. D. Marion, L. E. Kay, S. W. Sparks, D. A. Torchia, and A. Bax, *J. Am. Chem. Soc.* **111**, 1515 (1989).
12. E. R. P. Zuiderweg and S. W. Fesik, *Biochemistry* **28**, 2387 (1989).
13. L. E. Kay, G. M. Clore, A. Bax, and A. M. Gronenborn, *Science* **249**, 411 (1990).
14. P. Guntert, W. Braun, M. Billeter, and K. Wüthrich, *J. Am. Chem. Soc.* **111**, 3997 (1989).
15. M. Nilges, G. M. Clore, and A. M. Gronenborn, *Biopolymers* **29**, 813 (1990).
16. T. D. Spitzer, G. E. Martin, R. C. Crouch, J. P. Shockcor, and B. T. Farmer II, *J. Magn. Reson.* **99**, 433 (1992).
17. B. T. Farmer II, *J. Magn. Reson.* **93**, 635 (1991).
18. D. R. Muhandiram, N. Farrow, G. Y. Xu, S. H. Smallcombe, and L. E. Kay, *J. Magn. Reson. B*, **102**, 317 (1993).
19. D. S. Garrett, R. Powers, A. M. Gronenborn, and M. Clore, *J. Magn. Reson.* **95**, 214 (1991).
20. B. K. John, D. Plant, P. Webb, and R. E. Hurd, *J. Magn. Reson.* **98**, 200 (1992).
21. M. A. McCoy and L. Mueller, *J. Am. Chem. Soc.* **114**, 2108 (1992).
22. M. A. McCoy and L. Mueller, *J. Magn. Reson.* **98**, 674 (1992).
23. A. J. Shaka, P. B. Barker, and R. Freeman, *J. Magn. Reson.* **64**, 547 (1985).
24. A. Bax, G. M. Clore, P. C. Driscoll, A. M. Gronenborn, M. Ikura, and L. E. Kay, *J. Magn. Reson.* **87**, 620 (1990).
25. A. J. Shaka, J. Keeler, T. Frenkel, and R. Freeman, *J. Magn. Reson.* **52**, 335 (1983).
26. D. Marion, M. Ikura, R. Tschudin, and A. Bax, *J. Magn. Reson.* **85**, 393 (1989).